

Bounding Singular Values of Convolutional Layers

Sahil Singla and Soheil Feizi

Computer Science Department
University of Maryland, College Park

Abstract

In deep neural networks, the spectral norm of the Jacobian of a layer bounds the factor by which the norm of a signal changes during forward or backward propagation. Spectral norm regularization has also been shown to improve the generalization and robustness of deep networks. However, existing methods to compute the spectral norm of the jacobian of convolution layers either rely on heuristics (but are efficient in computation) or are exact (but computationally expensive to be used during training). In this work, we resolve these issues by deriving an upper bound on the spectral norm of a standard 2D multi-channel convolution layer. Our method provides a provable bound that is differentiable and can be computed efficiently during training with negligible overhead. We show that our spectral bound is an effective regularizer and can be used to bound the lipschitz constant and the curvature (eigenvalues of the Hessian) of neural network. Through experiments on MNIST and CIFAR-10, we demonstrate the effectiveness of our spectral bound in improving the generalization and provable robustness of deep networks against adversarial examples. Our code is available at <https://github.com/singlasahil14/CONV-SV>.

1 Introduction

Bounding the singular values of different layers of a neural network is a way to control the complexity of the model and has been used in different problems including robustness, generalization, optimization, generative modeling etc. For example, the spectral norm (the maximum singular value) of a layer bound the factor by which the norm of the signal increases or decreases during both forward and backward propagation within that layer. If all singular values are all close to one, then the gradients neither explode nor vanish [1, 2, 3]. Previous work has shown that the generalization error of the network can be bounded by the Lipschitz constant of the network [4, 5] which in turn can be bounded by the product of the spectral norm of the layers. Therefore, bounding the singular values can enhance the generalization of the network. Lipschitz constraint on the neural network is also known to be useful for Wasserstein distance estimation [6, 7, 8] which in turn can be used for generative models such as Wasserstein GANs[9, 10], Wasserstein VAEs[11] etc. Some previous works have also tried to certify robustness of neural networks against adversarial attacks by bounding the Lipschitz constant of the network [8, 12, 13, 14, 15, 16]. These considerations have resulted in multiple works to regularize neural networks by penalizing the spectral norm of the network layers [17, 18, 19, 20, 21].

For a fully connected layer with weights \mathbf{W} and bias \mathbf{b} , the lipschitz constant is simply given by spectral norm of the weight matrix i.e, $\|\mathbf{W}\|_2$, which can be computed efficiently using the power iteration method [22]. In particular, if the matrix \mathbf{W} is of size $p \times q$, the running complexity of power iteration (assuming convergence in constant number of steps) is $\mathcal{O}(pq)$.

Convolution layers [23] are one of the key components of modern neural networks, particularly in computer vision [24]. Given a convolution filter \mathbf{L} of dimensions $c_{out} \times c_{in} \times h \times w$ (h, w, c_{in}, c_{out} denote the height, width, number of input, output channels respectively) and a square input sample of size $c_{in} \times n \times n$ (the height and width are n), a naive representation of the Jacobian of this layer will result in a matrix of size $n^2 c_{out} \times n^2 c_{in}$. For example, for a typical convolution layer with the filter size $7 \times 7 \times 64 \times 3$ and Imagenet [25] sized input $3 \times 224 \times 224$, the corresponding jacobian matrix has a very large size: 802816×150528 . This makes the computation of spectral norm using the power iteration difficult. Furthermore, due to the structure of convolution operation, the jacobian will be a sparse matrix. But a naive computation of the

gradient using the outer product of singular vectors (corresponding to the largest singular value) will result in non-zero gradient at locations that are identically zero throughout training.

Recently, Sedghi et al. [21] has provided a principled approach to exactly compute the singular values of convolution layers. However, the method proposed in [21] is still computationally expensive prohibiting its use during the training of deep networks. In particular, their method requires the computation of the norm of n^2 matrices of size $c_{out} \times c_{in}$ (here n is the width and height of the input) for every convolution layer. Thus to compute the spectral norm of the convolution filter discussed in the previous paragraph, their method will compute the norm of $224 \times 224 = 50176$ matrices, each of size 64×3 . (see Table 1 for the running time). This makes their method prohibitively expensive to use during training. Moreover, computing the gradient of the spectral norm using this method is not straightforward. Thus, they compute all the singular values and clip above a certain threshold to bound the spectral norm of the layer.

Because of the aforementioned issues, efficient methods to control the spectral norm of convolution layers have resorted to heuristics and approximations [18, 19, 20, 26]. Typically they reshape the convolution filter of dimensions $c_{out} \times c_{in} \times h \times w$ to construct a matrix of dimensions $c_{out} \times hwc_{in}$, and use the spectral norm of this matrix as a (heuristic) estimate of the spectral norm of the convolution layer. To regularize during training, they use the outer product of the corresponding singular vectors as the gradient of the largest singular value with respect to the reshaped matrix. Since the weights do not change significantly during each training step, they use one iteration of power method during each step to update the singular values and vectors (using the singular vectors computed in the previous training step). This method generally results in negligible overhead during training, however it does not have any theoretical underpinnings.

Filter shape	Spectral norm estimates			Running time (in seconds)		
	Exact method [21]	Heuristic method [19]	Upper bound (Ours)	Exact	Heuristic	Ours
$64 \times 3 \times 7 \times 7$	15.917	4.128	46.373	3.166	0.003	0.280
$64 \times 64 \times 3 \times 3$	6.006	3.109	9.545	75.481	0.004	0.007
$64 \times 64 \times 3 \times 3$	5.341	2.163	6.296	80.777	0.003	0.008
$64 \times 64 \times 3 \times 3$	6.999	2.934	8.712	80.213	0.004	0.008
$64 \times 64 \times 3 \times 3$	3.816	1.937	5.402	81.744	0.004	0.008
$128 \times 64 \times 3 \times 3$	4.706	1.978	6.923	30.634	0.007	0.010

Table 1: Comparison between the exact spectral norm of the jacobian $\|\mathbf{J}\|_2$ (computed using Sedghi et al. [21]), the heuristic method [19, 20] and our proposed bound $\min(\sqrt{hw}\|\mathbf{R}\|_2, \sqrt{hw}\|\mathbf{S}\|_2)$ for the first 6 layers of a Resnet-18 network pretrained on Imagenet [25]. The heuristic is always significantly smaller than the exact spectral norm. However, $\min(\sqrt{hw}\|\mathbf{R}\|_2, \sqrt{hw}\|\mathbf{S}\|_2)$ is within 1.5 times the exact spectral norm $\|\mathbf{J}\|_2$ (except the first layer). All running times were computed on the CPU using tensorflow. Results for all layers in Appendix Table 7. We observe a similar trend.

On one hand, there is a computationally efficient but heuristic way of computing and bounding the spectral norm of convolutional layers [19, 20]. However in Table 1, we show that this heuristic estimate can be very small compared to the exact spectral norm for a standard Resnet-18 architecture [27] pretrained on Imagenet [25]. On the other hand, the exact computation of the spectral norm of convolutional layers proposed by Sedghi et al. [21] can be very expensive for commonly used architectures. For example, Table 1 shows the running time of the method proposed in [21].

In this paper, we resolve these issues by deriving a differentiable and efficient upper bound on the spectral norm of convolutional layers. Our bound is provable and *not* based on heuristics. Moreover, our computational complexity is similar to that of Miyato et al. [19, 20] allowing our bound to be used as a regularizer for efficiently training deep convolutional networks. In this way, our proposed approach combines the benefits of the speed of the heuristic approach and the rigor of the approach by Sedghi et al. [21]. Table 2 summarizes the differences between previous work and our approach.

	Exact (Sedghi et al.[21])	Heuristic (Miyato et al.[19])	Upper bound (Ours)
Computation	Norm of n^2 matrices, each of size $c_{out} \times c_{in}$	Norm of one matrix of size $c_{out} \times (c_{in}wh)$	Norm of one matrix of size $(c_{out}h) \times (c_{in}w)$
Running time	$\mathcal{O}(n^2 c_{out} c_{in})$	$\mathcal{O}(h w c_{out} c_{in})$	$\mathcal{O}(h w c_{out} c_{in})$
Principled bound	✓	✗	✓

Table 2: Comparison of various methods used for computing the norm of convolution layers. n is the height and width for a square input, c_{in} is the number of input channels, c_{out} is the number of output channels, h and w are the height and width of the convolution filter.

Below we briefly explain our main result. Consider a convolution filter \mathbf{L} of dimensions $c_{out} \times c_{in} \times h \times w$ and input of size $c_{in} \times n \times n$. The corresponding jacobian matrix \mathbf{J} is of size $n^2 c_{out} \times n^2 c_{in}$. We show that the largest singular value of the jacobian i.e $\|\mathbf{J}\|_2$ is bounded as follows:

$$\|\mathbf{J}\|_2 \leq \min\left(\sqrt{hw}\|\mathbf{R}\|_2, \sqrt{hw}\|\mathbf{S}\|_2\right)$$

where \mathbf{R} and \mathbf{S} are matrices of sizes $hc_{out} \times wc_{in}$ and $wc_{out} \times hc_{in}$, respectively, and can be computed by appropriately reshaping the filter \mathbf{L} (details in Section 3). Also note that the usual heuristic would reshape \mathbf{L} to a matrix of size $c_{out} \times hwc_{in}$ in contrast to matrices \mathbf{R} and \mathbf{S} of sizes $hc_{out} \times wc_{in}$ and $wc_{out} \times hc_{in}$, respectively. Further note that this upper bound is independent of the input width and height (n). Formal results are stated in Theorem 1 and proved in Appendix Section A. This leads to an extremely efficient method to compute the spectral norm of convolution layers using the following numpy code:

```
def SingularValuesBound(kernel):
    c_out, c_in, h, w = kernel.shape
    kernel_transpose = np.transpose(kernel, (0, 2, 1, 3))
    kernel_matrix = np.reshape(kernel_transpose, (h*c_out, -1))
    return (np.sqrt(h*w)*np.linalg.norm(kernel_matrix, ord=2))
```

Code is available at <https://github.com/singlasahil14/CONV-SV>.

2 Notation

For a vector \mathbf{v} , we use \mathbf{v}_j to denote the element in the j^{th} position of the vector. We use $\mathbf{A}_{j,:}$ to denote the j^{th} row of the matrix \mathbf{A} , $\mathbf{A}_{:,k}$ to denote the k^{th} column of the matrix \mathbf{A} . We assume both $\mathbf{A}_{j,:}$ and $\mathbf{A}_{:,k}$ to be column vectors (thus $\mathbf{A}_{j,:}$ is constructed by taking the transpose of j^{th} row of \mathbf{A}). $\mathbf{A}_{j,k}$ denotes the element in j^{th} row and k^{th} column of \mathbf{A} . $\mathbf{A}_{j,:k}$ and $\mathbf{A}_{:j,k}$ denote the vectors containing the first k elements of the j^{th} row and first j elements of k^{th} column, respectively. $\mathbf{A}_{:,k}$ denotes the matrix containing the first j rows and k columns of \mathbf{A} :

$$\mathbf{A}_{j,:k} = \begin{bmatrix} \mathbf{A}_{j,0} \\ \mathbf{A}_{j,1} \\ \vdots \\ \mathbf{A}_{j,k-1} \end{bmatrix}, \quad \mathbf{A}_{:j,k} = \begin{bmatrix} \mathbf{A}_{0,k} \\ \mathbf{A}_{1,k} \\ \vdots \\ \mathbf{A}_{j-1,k} \end{bmatrix}, \quad \mathbf{A}_{:,k} = \begin{bmatrix} \mathbf{A}_{0,0} & \mathbf{A}_{0,1} & \cdots & \mathbf{A}_{0,k-1} \\ \mathbf{A}_{1,0} & \mathbf{A}_{1,1} & \cdots & \mathbf{A}_{1,k-1} \\ \vdots & \vdots & \ddots & \vdots \\ \mathbf{A}_{j-1,0} & \mathbf{A}_{j-1,1} & \cdots & \mathbf{A}_{j-1,k-1} \end{bmatrix}$$

For $n \in \mathbb{N}$, we use $[n]$ to denote the set $\{0, \dots, n\}$ and $[p, q]$ ($p < q$) to denote the set $\{p, p+1, \dots, q\}$. We will index the rows and columns of matrices using elements of $[n]$, i.e. numbering from 0. Addition of row and column indices will be done mod n unless otherwise indicated. For a matrix $\mathbf{A} \in \mathbb{R}^{q \times r}$ and a tensor $\mathbf{B} \in \mathbb{R}^{p \times q \times r}$, $vec(\mathbf{A})$ denotes the vector constructed by stacking the rows of \mathbf{A} and $vec(\mathbf{B})$ denotes the vector constructed by stacking the vectors $vec(\mathbf{B}_{j,:,:})$, $j \in [p-1]$:

$$vec(\mathbf{A}) = \begin{bmatrix} \mathbf{A}_{0,:} \\ \mathbf{A}_{1,:} \\ \vdots \\ \mathbf{A}_{q-1,:} \end{bmatrix}, \quad vec(\mathbf{B}) = \begin{bmatrix} vec(\mathbf{B}_{0,:,:}) \\ vec(\mathbf{B}_{1,:,:}) \\ \vdots \\ vec(\mathbf{B}_{p-1,:,:}) \end{bmatrix}$$

For a given vector $\mathbf{v} \in \mathbb{R}^n$, $\text{circ}(\mathbf{v})$ denotes the $n \times n$ circulant matrix constructed from \mathbf{v} i.e rows of $\text{circ}(\mathbf{v})$ are circular shifts of \mathbf{v} . For a matrix $\mathbf{A} \in \mathbb{R}^{n \times n}$, $\text{circ}(\mathbf{A})$ denotes the $n^2 \times n^2$ doubly block circulant matrix constructed from \mathbf{A} , i.e each $n \times n$ block of $\text{circ}(\mathbf{A})$ is a circulant matrix constructed from the rows $\mathbf{A}_{j,:}$, $j \in [n-1]$:

$$\text{circ}(\mathbf{v}) = \begin{bmatrix} \mathbf{v}_0 & \mathbf{v}_1 & \cdots & \mathbf{v}_{n-1} \\ \mathbf{v}_{n-1} & \mathbf{v}_0 & \cdots & \mathbf{v}_{n-2} \\ \vdots & \vdots & \ddots & \vdots \\ \mathbf{v}_1 & \mathbf{v}_2 & \cdots & \mathbf{v}_0 \end{bmatrix}, \quad \text{circ}(\mathbf{A}) = \begin{bmatrix} \text{circ}(\mathbf{A}_{0,:}) & \text{circ}(\mathbf{A}_{1,:}) & \cdots & \text{circ}(\mathbf{A}_{n-1,:}) \\ \text{circ}(\mathbf{A}_{n-1,:}) & \text{circ}(\mathbf{A}_{0,:}) & \cdots & \text{circ}(\mathbf{A}_{n-2,:}) \\ \vdots & \vdots & \ddots & \vdots \\ \text{circ}(\mathbf{A}_{1,:}) & \text{circ}(\mathbf{A}_{2,:}) & \cdots & \text{circ}(\mathbf{A}_{0,:}) \end{bmatrix}$$

We use \mathbf{F} to denote the Fourier matrix of dimensions $n \times n$, i.e $\mathbf{F}_{j,k} = \omega^{jk}$, $\omega = e^{-2\pi i/n}$, $i^2 = -1$. For a matrix \mathbf{A} , $\sigma(\mathbf{A})$ denotes the set of singular values of \mathbf{A} . $\sigma_{max}(\mathbf{A})$ and $\sigma_{min}(\mathbf{A})$ denotes the largest and smallest singular values of \mathbf{A} respectively. $\mathbf{A} \otimes \mathbf{B}$ denotes the kronecker product of \mathbf{A} and \mathbf{B} . We use $\mathbf{A} \odot \mathbf{B}$ to denote the hadamard product between two matrices (or vectors) of the same size. We use \mathbf{I}_n to denote the identity matrix of dimensions $n \times n$.

We use the following notation for a convolutional neural network. L denotes the number of layers and ϕ denotes the activation function. For an input \mathbf{x} , we use $\mathbf{z}^{(I)}(\mathbf{x}) \in \mathbb{R}^{N_I}$ and $\mathbf{a}^{(I)}(\mathbf{x}) \in \mathbb{R}^{N_I}$ to denote the input (*before* applying the activation function) and output (*after* applying the activation function) of neurons in the I^{th} hidden layer of the network, respectively. Thus $\mathbf{a}^{(0)}$ denotes the input image \mathbf{x} . To simplify notation and when no confusion arises, we make the dependency of $\mathbf{z}^{(I)}$ and $\mathbf{a}^{(I)}$ to \mathbf{x} implicit. $\phi'(\mathbf{z}^{(I)})$ and $\phi''(\mathbf{z}^{(I)})$ denotes the elementwise derivative and double derivative of ϕ at $\mathbf{z}^{(I)}$. $\mathbf{W}^{(I)}$ denotes the weights for the I^{th} layer i.e $\mathbf{W}^{(I)}$ will be a tensor for a convolution layer and a matrix for a fully connected layer. $\mathbf{J}^{(I)}$ denotes the jacobian matrix of $\text{vec}(\mathbf{z}^{(I)})$ with respect to the input \mathbf{x} . θ denotes the neural network parameters. $f_\theta(\mathbf{x})$ denotes the softmax probabilities output by the network for an input \mathbf{x} . For an input \mathbf{x} and label y , the cross entropy loss is denoted by $\ell(f_\theta(\mathbf{x}), y)$.

3 Main Result

Consider a convolution filter \mathbf{L} of size $c_{out} \times c_{in} \times h \times w$ applied to an input \mathbf{X} of size $c_{in} \times n \times n$. The filter \mathbf{L} takes an input patch of size $c_{in} \times h \times w$ from the input and outputs a vector of size c_{out} for every such patch. The same operation is applied across all such patches in the image. To apply convolution at the edges of the image, modern convolution layers either not compute the outputs thus reducing the size of the feature map, or pad the input with zeros to preserve its size. When we pad with zeroes, the corresponding jacobian becomes a *topelitz matrix*.

Another version of convolution treats the input as if it were a torus; when the convolution operation calls for a pixel that is off the right end of the image, the layer "wraps around" to take it from the left edge, and similarly for the other edges. For this version of convolution, the jacobian is a *circulant matrix*. The quality of approximation between a toepnitz and circulant matrix has been heavily analyzed in the case of 1D [28] and 2D signals [29]. For the 2D case (similar to the 1D case), $O(1/p)$ bound is obtained on the error, where $p \times p$ is the size of both (topelitz and circulant) matrices. Consequently, theoretical analysis of convolutions that wrap around has been become standard. This is the case that we analyze in this work. Furthermore, we assume the stride size to be 1 in both horizontal and vertical directions.

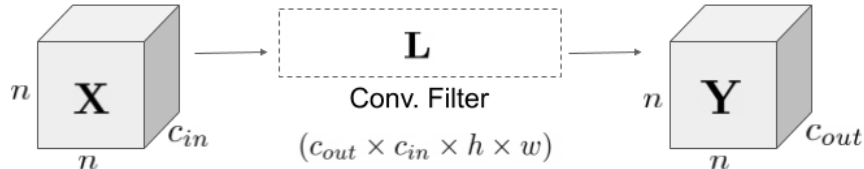


Figure 1: For an input \mathbf{X} , a convolution filter \mathbf{L} is applied to give output \mathbf{Y} .

Thus, the corresponding output \mathbf{Y} produced from applying the filter \mathbf{L} to input \mathbf{X} is of size $c_{out} \times n \times n$.

The corresponding jacobian (\mathbf{J}) will be a matrix of size $n^2 c_{out} \times n^2 c_{in}$ satisfying:

$$\text{vec}(\mathbf{Y}) = \mathbf{J} \text{vec}(\mathbf{X})$$

Our goal is to bound the norm of jacobian of the convolution operation i.e $\|\mathbf{J}\|_2$.

Sedghi et al.[21] also derive an expression for the exact singular values of the jacobian of convolution layers. However, their method requires the computation of the spectral norm of n^2 matrices (each matrix of size $c_{out} \times c_{in}$) for every convolution layer making it impractical to use during training.

In this work, we show that it is possible to construct a matrix $\mathbf{G}^{(j,k)}$ parametrized by the Fourier vectors $\mathbf{F}_{:,j}, \mathbf{F}_{:,k}$ such that for each j and k , singular values of $\mathbf{G}^{(j,k)}$ are a subset of the singular values of the jacobian \mathbf{J} . Specifically, the matrix $\mathbf{G}^{(j,k)}$ is given by the following equations:

$$\mathbf{G}^{(j,k)} = (\mathbf{I}_{c_{out}} \otimes (\mathbf{F}_{:h,j})^T) \mathbf{R} (\mathbf{I}_{c_{in}} \otimes \mathbf{F}_{:w,k}) = (\mathbf{I}_{c_{out}} \otimes (\mathbf{F}_{:w,k})^T) \mathbf{S} (\mathbf{I}_{c_{in}} \otimes \mathbf{F}_{:h,j})$$

where \mathbf{R} and \mathbf{S} are matrices of sizes $c_{out}h \times c_{in}w$ and $c_{out}w \times c_{in}h$ defined as follows:

$$\mathbf{R} = \begin{bmatrix} \mathbf{L}_{0,0,:} & \mathbf{L}_{0,1,:} & \cdots & \mathbf{L}_{0,c_{in}-1,:} \\ \mathbf{L}_{1,0,:} & \mathbf{L}_{1,1,:} & \cdots & \mathbf{L}_{1,c_{in}-1,:} \\ \vdots & \vdots & \ddots & \vdots \\ \mathbf{L}_{c_{out}-1,0,:} & \mathbf{L}_{c_{out}-1,1,:} & \cdots & \mathbf{L}_{c_{out}-1,c_{in}-1,:} \end{bmatrix}, \quad \mathbf{S} = \begin{bmatrix} (\mathbf{L}_{0,0,:})^T & \cdots & (\mathbf{L}_{0,c_{in}-1,:})^T \\ (\mathbf{L}_{1,0,:})^T & \cdots & (\mathbf{L}_{1,c_{in}-1,:})^T \\ \vdots & \ddots & \vdots \\ (\mathbf{L}_{c_{out}-1,0,:})^T & \cdots & (\mathbf{L}_{c_{out}-1,c_{in}-1,:})^T \end{bmatrix} \quad (1)$$

Using the property of kronecker product $\|\mathbf{A} \otimes \mathbf{B}\|_2 = \|\mathbf{A}\|_2 \|\mathbf{B}\|_2$, we have:

$$\begin{aligned} \|\mathbf{I}_{c_{out}} \otimes (\mathbf{F}_{:h,j})^T\|_2 &= \|\mathbf{I}_{c_{in}} \otimes \mathbf{F}_{:h,j}\|_2 = \|\mathbf{F}_{:h,j}\|_2 \leq \sqrt{h} \\ \|\mathbf{I}_{c_{in}} \otimes \mathbf{F}_{:w,k}\|_2 &= \|\mathbf{I}_{c_{out}} \otimes (\mathbf{F}_{:w,k})^T\|_2 = \|\mathbf{F}_{:w,k}\|_2 \leq \sqrt{w} \end{aligned}$$

Thus, taking the norm of $\mathbf{G}^{(j,k)}$ and using the above properties, we get the following theorem:

Theorem 1 Consider a convolution filter \mathbf{L} of size $c_{out} \times c_{in} \times h \times w$ that applied to input \mathbf{X} of size $c_{in} \times n \times n$ gives output \mathbf{Y} of size $c_{out} \times n \times n$. The jacobian of \mathbf{Y} with respect to \mathbf{X} (call it \mathbf{J}) will be a matrix of size $n^2 c_{out} \times n^2 c_{in}$. The spectral norm of \mathbf{J} is bounded by:

$$\|\mathbf{J}\|_2 \leq \min\left(\sqrt{hw} \|\mathbf{R}\|_2, \sqrt{hw} \|\mathbf{S}\|_2\right)$$

where \mathbf{R} and \mathbf{S} are matrices defined in equation (1).

Proof is presented in the Appendix Section A.

In the current literature [19], the heuristic used for estimating the spectral norm involves combining the dimensions of sizes h, w, c_{in} in the filter \mathbf{L} to create a matrix of dimensions $c_{out} \times hwc_{in}$. The norm of resulting matrix is used as a heuristic estimate of the spectral norm of the jacobian of convolution operator. This is motivated by the fact that convolution filter outputs a vector of size c_{out} for each input patch of size $c_{in} \times h \times w$. However, as we show in Table 1, this is not a correct way of bounding the spectral norm of the convolutional layer. Theorem 1 proves that the correct bound would instead combine the dimensions of sizes h and c_{out} or equivalently w and c_{out} in the filter. The norm of this matrix multiplied with a factor of \sqrt{hw} gives a provable upper bound on the singular values of the jacobian.

3.1 Gradient Computation

Since the matrix \mathbf{R} can be directly computed by reshaping the filter weights \mathbf{L} (equation (1)), we can compute the derivative of our bound $\sqrt{hw} \|\mathbf{R}\|_2$ (or $\sqrt{hw} \|\mathbf{S}\|_2$) with respect to filter weights \mathbf{L} by first computing the derivative of $\sqrt{hw} \|\mathbf{R}\|_2$ with respect to \mathbf{R} and then appropriately reshaping the derivative obtained.

Let \mathbf{u} and \mathbf{v} be the singular vectors corresponding to the largest singular value i.e $\|\mathbf{R}\|_2$, then the derivative of our upper bound $\sqrt{hw} \|\mathbf{R}\|_2$ with respect to \mathbf{R} can be computed as follows:

$$\nabla_{\mathbf{R}} \sqrt{hw} \|\mathbf{R}\|_2 = \sqrt{hw} \mathbf{u} \mathbf{v}^T \quad \text{where } \|\mathbf{R}\|_2 = \mathbf{u}^T \mathbf{R} \mathbf{v}$$

Moreover since the weights do not change significantly during training, we can use 1 iteration of power method to update \mathbf{u}, \mathbf{v} and $\|\mathbf{R}\|_2$ during each training step (similar to Miyato et al. [19, 20]). This allows us to use our bound as a regularizer during training.

4 Experiments

4.1 Comparison with existing methods

In Table 1, we show a comparison between the exact spectral norm (computed using Sedghi et al.[21]), the heuristic method of [19, 20] and our upper bound i.e $\min(\sqrt{hw}\|\mathbf{R}\|_2, \sqrt{hw}\|\mathbf{S}\|_2)$ on a pre-trained Resnet-18 network [27]. Except for the first layer, we observe that our bound is within 1.5 times the value of the exact spectral norm while being significantly faster to compute. However, the heuristic method of [19, 20] is significantly smaller than $\|\mathbf{J}\|_2$ for all layers. In Appendix Table 6, we observe that both elements of our proposed bound (i.e. $\sqrt{hw}\|\mathbf{R}\|_2$ and $\sqrt{hw}\|\mathbf{S}\|_2$) are close to each other (but not equal). Thus, by taking the minimum of the two, we can get a small gain.

4.2 Effect on generalization

In Table 3, we study the effect of using our proposed bound as a regularizer on the generalization error. Since we empirically observe a small difference between the two components of our bound (i.e. $\sqrt{hw}\|\mathbf{R}\|_2$ and $\sqrt{hw}\|\mathbf{S}\|_2$), we use $\sqrt{hw}\|\mathbf{R}\|_2$ for regularization. We use a Resnet-32 neural network architecture and the CIFAR-10 dataset [30] for training. For regularization, we use the sum of spectral norms of all layers of the network during training. Thus our regularized objective function is given as follows:

$$\min_{\theta} \mathbb{E}_{(\mathbf{x}, y)} [\ell(f_{\theta}(\mathbf{x}), y)] + \beta \sum_I u^{(I)} \quad (2)$$

where β is the regularization coefficient, (\mathbf{x}, y) are the input-label pairs in the training data, $u^{(I)}$ denotes the bound for the I^{th} linear (convolution or fully connected) layer. For the convolution layers, $u^{(I)}$ is computed as $\sqrt{hw}\|\mathbf{R}\|_2$ using Theorem 1. For the fully connected layers, we can compute $u^{(I)}$ using power iteration[19, 20].

Note that weight decay [31] is indirectly minimizing the Frobenius norm squared which is equal to the sum of squares of singular values. Thus, it implicitly forces the largest singular values for each layer (i.e the spectral norm) to be small. Therefore, to measure the effect of our regularizer on the test set accuracy, we compare the effect of adding our regularizer both with and without weight decay.

Our experimental results are reported in Table 3. For the case of no weight decay, we observe an improvement of 0.95% over the case when $\beta = 0$. When we include a weight decay of 10^{-4} in training, there is an improvement of 0.7% over the baseline. We note that [21] show an improvement of 0.9% using clipping of singular values above a certain threshold. However, since their method requires the computation of all singular values, it is significantly more time consuming compared to ours which results in negligible overhead. We report the running time of these methods in Table 1.

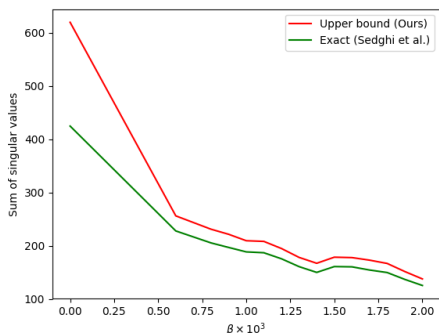


Figure 2: We plot the effect of increasing β on the sum of the bounds (computed using our method i.e $\sqrt{hw}\|\mathbf{R}\|_2$) and sum of true spectral norms ($\|\mathbf{J}^{(I)}\|_2$ computed using Sedghi et al.[21]) for a Resnet-32 neural network trained on CIFAR-10 dataset (without any weight decay). We observe that the gap between the two decreases as we increase β . In Appendix Table 5, we show the effect of increasing β on the bounds of individual layers of the same network.)

4.3 Effect on robustness

A robustness certificate against adversarial examples is the minimum distance (or a lower bound) of a given input to the decision boundary of the classifier. For *any* perturbation of the input with a magnitude smaller

β	Test accuracy (No weight decay)	Test accuracy (weight decay = 10^{-4})
0	91.26%	92.53%
0.0008	91.61%	92.87%
0.0009	91.77%	93.00%
0.0010	91.70%	93.13%
0.0011	91.67%	92.88%
0.0012	91.35%	92.67%
0.0013	91.51%	92.89%
0.0014	92.18%	92.89%
0.0015	91.69%	93.05%
0.0016	92.02%	92.76%
0.0017	91.50%	93.20%
0.0018	91.58%	91.67%
0.0019	92.00%	92.52%
0.0020	91.34%	92.71%

Table 3: Effect of our proposed regularizer on test accuracy on CIFAR-10 dataset for a Resnet-32 network

than the certificate, the classification output will provably remain unchanged. Computing exact robustness certificates for deep classifiers is difficult in general since it requires solving a non-convex optimization. However, recent work [32] shows that using a global upper bound on the largest eigenvalue of the Hessian (with respect to the input) as a regularizer during training results in provable robustness against adversarial examples (for the l_2 metric). Specifically, the authors derive a closed form expression for the Hessian of a deep network and use the global upper bound on the spectral norm of the same expression as a regularizer during training. Using Lemma 1 in [32], we know that for a two-layer (or equivalently one-hidden layer) network, the Hessian of the i^{th} logit of the neural network with respect to the input \mathbf{x} is given by the following expression:

$$\nabla_{\mathbf{x}}^2 \mathbf{z}_i^{(2)} = (\mathbf{J}^{(1)})^T \text{diag} \left[\mathbf{W}_{i,:}^{(2)} \odot \phi''(\text{vec}(\mathbf{z}^{(1)})) \right] \mathbf{J}^{(1)}$$

Furthermore using Theorem 3 in the same work, we also know that if the double derivative the activation function ϕ is globally bounded (a condition satisfied for popular activation functions such as sigmoid, tanh, softplus) i.e:

$$|\phi''(x)| \leq b \quad \forall x \in \mathbb{R} \quad (3)$$

The upper bound on the spectral norm of the hessian matrix (or equivalently the bounds on the eigenvalues of the hessian) is simply given by:

$$\left\| \nabla_{\mathbf{x}}^2 \mathbf{z}_i^{(2)} \right\|_2 \leq b \|\mathbf{J}^{(1)}\|_2^2 \max_j \left(|\mathbf{W}_{i,j}^{(2)}| \right), \quad \forall \mathbf{x} \quad (4)$$

Thus for label y and adversarial target t , the curvature bound on the difference between logits ($\mathbf{z}_y^{(2)} - \mathbf{z}_t^{(2)}$) is derived by replacing $\mathbf{W}_{i,j}^{(2)}$ with $\mathbf{W}_{y,j}^{(2)} - \mathbf{W}_{t,j}^{(2)}$ in inequality (4):

$$\left\| \nabla_{\mathbf{x}}^2 \left(\mathbf{z}_y^{(2)} - \mathbf{z}_t^{(2)} \right) \right\|_2 \leq b \|\mathbf{J}^{(1)}\|_2^2 \max_j \left(|\mathbf{W}_{y,j}^{(2)} - \mathbf{W}_{t,j}^{(2)}| \right), \quad \forall \mathbf{x}$$

Due to the difficulty of computing $\|\mathbf{J}^{(l)}\|_2$ when the I^{th} layer is a convolution, the authors restrict their analysis to fully connected networks where $\mathbf{J}^{(l)}$ simply equals the I^{th} layer weight matrix. However using

Theorem 1, we can further bound $\mathbf{J}^{(I)}$ and run similar experiments for the convolution layers. Thus for a 2 layer convolution network, our regularized objective function is given as follows:

$$\min_{\theta} \mathbb{E}_{(\mathbf{x}, y)} [\ell(f_{\theta}(\mathbf{x}), y)] + \gamma b \max_j (|\mathbf{W}_{y,j}^{(2)} - \mathbf{W}_{t,j}^{(2)}|) (u^{(1)})^2 \quad (5)$$

where γ is the regularization coefficient, (\mathbf{x}, y) are the input-label pairs in the training data, $u^{(I)}$ denotes the bound on the spectral norm for the I^{th} linear (convolution or fully connected) layer. For the convolutional layer (i.e the first layer), $u^{(1)}$ is again computed as $\sqrt{hw} \|\mathbf{R}\|_2$ using Theorem 1.

In Table 4, we study the effect of the regularization coefficient γ on robustness of a 2 layer convolutional neural network with the softplus [33] activation function when trained with CRT [32]. We assume l_2 norm bounded adversarial perturbations of size 0.5. We achieve certified accuracy of 91.47% on MNIST dataset and 29.26% on CIFAR-10 dataset. We further observe that adversarial training using CRT [32] (without any curvature regularization i.e $\gamma = 0$) results in zero certified robust accuracy. However curvature regularization significantly boosts certified robustness. Empirical robust accuracy is computed by running l_2 bounded PGD (200 steps, step size 0.01). Certified Robust Accuracy is computed as the fraction of correctly classified samples with CRC [32] greater than 0.5. We use convolution layer with 64 filters and stride of size 2. To the best of our knowledge, this is the first work that derives a non-trivial certified robust accuracy on a single hidden layer network with differentiable activation function.

γ	MNIST			CIFAR-10		
	Standard Accuracy	Empirical Robust Accuracy	Certified Robust Accuracy	Standard Accuracy	Empirical Robust Accuracy	Certified Robust Accuracy
0	98.68%	87.81%	0.00%	56.22%	14.88%	0.00%
0.005	97.67%	93.71%	91.47%	56.18%	30.19%	9.37%
0.01	97.08%	92.92%	91.25%	53.52%	31.82%	17.39%
0.02	96.36%	90.98%	89.58%	49.55%	31.80%	25.93%
0.03	95.54%	89.99%	88.75%	46.56%	31.98%	29.26%

Table 4: Comparison between certified robust accuracy for different values of the regularization parameter γ for a single hidden layer convolutional neural network with softplus activation function

5 Conclusion

In this paper, we derive an efficient method to compute an upper bound on the spectral norm of convolution layers. We show that using the same bound as a regularizer during training results in lower test error on the CIFAR-10 dataset. We also show that the same bound can be used to bound the eigenvalues of the Hessian (the curvature) of a deep neural network. By regularizing the curvature, we achieve non-trivial certified robustness on a 2 layer CNN for MNIST and CIFAR-10 dataset. Since it is also known that Lipschitz constraint on a neural network is useful for generalization bounds, provable adversarial robustness and the Wasserstein distance estimation, this opens up the possibility of several avenues of future research.

References

- [1] Sepp Hochreiter. Untersuchungen zu dynamischen neuronalen netzen. 1991.
- [2] Sepp Hochreiter and Yoshua Bengio. Gradient flow in recurrent nets: the difficulty of learning long-term dependencies. 2001.
- [3] Guenter Klambauer, Thomas Unterthiner, Andreas Mayr, and Sepp Hochreiter. Self-normalizing neural networks. In *NIPS*, 2017.

- [4] Peter L. Bartlett, Dylan J. Foster, and Matus Telgarsky. Spectrally-normalized margin bounds for neural networks. In *Proceedings of the 31st International Conference on Neural Information Processing Systems*, NIPS'17, pages 6241–6250, USA, 2017. Curran Associates Inc.
- [5] Philip M. Long and Hanie Sedghi. Size-free generalization bounds for convolutional neural networks, 2019.
- [6] Gabriel Peyr and Marco Cuturi. Computational optimal transport, 2018.
- [7] Qiyang Li, Saminul Haque, Cem Anil, James Lucas, Roger Grosse, and Jrn-Henrik Jacobsen. Preventing gradient attenuation in lipschitz constrained convolutional networks, 2019.
- [8] Cem Anil, James Lucas, and Roger B. Grosse. Sorting out lipschitz function approximation. In *ICML*, 2018.
- [9] Martin Arjovsky, Soumith Chintala, and Lon Bottou. Wasserstein gan, 2017.
- [10] Ishaan Gulrajani, Faruk Ahmed, Martin Arjovsky, Vincent Dumoulin, and Aaron Courville. Improved training of wasserstein gans, 2017.
- [11] Ilya Tolstikhin, Olivier Bousquet, Sylvain Gelly, and Bernhard Schoelkopf. Wasserstein auto-encoders, 2017.
- [12] Christian Szegedy, Wojciech Zaremba, Ilya Sutskever, Joan Bruna, Dumitru Erhan, Ian Goodfellow, and Rob Fergus. Intriguing properties of neural networks. In *International Conference on Learning Representations*, 2014.
- [13] Jonathan Peck, Joris Roels, Bart Goossens, and Yvan Saeys. Lower bounds on the robustness to adversarial perturbations. In *NIPS*, 2017.
- [14] Huan Zhang, Tsui-Wei Weng, Pin-Yu Chen, Cho-Jui Hsieh, and Luca Daniel. Efficient neural network robustness certification with general activation functions. *ArXiv*, abs/1811.00866, 2018.
- [15] Matthias Hein and Maksym Andriushchenko. Formal guarantees on the robustness of a classifier against adversarial manipulation. In I. Guyon, U. V. Luxburg, S. Bengio, H. Wallach, R. Fergus, S. Vishwanathan, and R. Garnett, editors, *Advances in Neural Information Processing Systems 30*, pages 2266–2276. 2017.
- [16] Moustapha Cisse, Piotr Bojanowski, Edouard Grave, Yann Dauphin, and Nicolas Usunier. Parseval networks: Improving robustness to adversarial examples. In *Proceedings of the 34th International Conference on Machine Learning - Volume 70*, ICML'17, pages 854–863. JMLR.org, 2017.
- [17] H. Drucker and Y. Le Cun. Improving generalization performance using double backpropagation. *Trans. Neur. Netw.*, 3(6):991–997, November 1992.
- [18] Yuichi Yoshida and Takeru Miyato. Spectral norm regularization for improving the generalizability of deep learning. *ArXiv*, abs/1705.10941, 2017.
- [19] Takeru Miyato, Toshiki Kataoka, Masanori Koyama, and Yuichi Yoshida. Spectral normalization for generative adversarial networks. In *International Conference on Learning Representations*, 2018.
- [20] Takeru Miyato, Shin ichi Maeda, Masanori Koyama, and Shin Ishii. Virtual adversarial training: A regularization method for supervised and semi-supervised learning. *IEEE Transactions on Pattern Analysis and Machine Intelligence*, 41:1979–1993, 2017.
- [21] Hanie Sedghi, Vineet Gupta, and Philip M Long. The singular values of convolutional layers. *arXiv preprint arXiv:1805.10408*, 2018.
- [22] Gene H. Golub and Charles F. Van Loan. *Matrix Computations (3rd Ed.)*. Johns Hopkins University Press, Baltimore, MD, USA, 1996.

- [23] Yann LeCun. Gradient-based learning applied to document recognition. 1998.
- [24] Alex Krizhevsky, Ilya Sutskever, and Geoffrey E. Hinton. Imagenet classification with deep convolutional neural networks. *Commun. ACM*, 60:84–90, 2012.
- [25] J. Deng, W. Dong, R. Socher, L. Li, Kai Li, and Li Fei-Fei. Imagenet: A large-scale hierarchical image database. In *2009 IEEE Conference on Computer Vision and Pattern Recognition*, pages 248–255, June 2009.
- [26] Henry Gouk, Eibe Frank, Bernhard Pfahringer, and Michael Cree. Regularisation of neural networks by enforcing lipschitz continuity, 2018.
- [27] Kaiming He, Xiangyu Zhang, Shaoqing Ren, and Jian Sun. Deep residual learning for image recognition. *2016 IEEE Conference on Computer Vision and Pattern Recognition (CVPR)*, pages 770–778, 2015.
- [28] Robert M. Gray. Toeplitz and circulant matrices: A review. *Commun. Inf. Theory*, 2(3):155–239, August 2005.
- [29] Z. Zhu and M. B. Wakin. On the asymptotic equivalence of circulant and toeplitz matrices. *IEEE Transactions on Information Theory*, 63(5):2975–2992, May 2017.
- [30] Alex Krizhevsky. Learning multiple layers of features from tiny images. Technical report, 2009.
- [31] Anders Krogh and John A. Hertz. A simple weight decay can improve generalization. In *NIPS*, 1991.
- [32] Anonymous. Curvature-based robustness certificates against adversarial examples. In *Submitted to International Conference on Learning Representations*, 2020. Under review.
- [33] Charles Dugas, Y. Bengio, Francois Blisle, Claude Nadeau, and Rene Garcia. Incorporating second-order functional knowledge for better option pricing. pages 472–478, 01 2000.

A Proof of Theorem 1

Proof Consider an input $\mathbf{X} \in \mathbb{R}^{c_{in} \times n \times n}$ and a convolution filter $\mathbf{L} \in \mathbb{R}^{c_{out} \times c_{in} \times h \times w}$ to \mathbf{X} such that $n > \max(h, w)$. Using \mathbf{L} , we construct a new filter $\mathbf{K} \in \mathbb{R}^{c_{out} \times c_{in} \times n \times n}$ by padding with zeroes:

$$\mathbf{K}_{c,d,k,l} = \begin{cases} \mathbf{L}_{c,d,k,l}, & k \in [h-1], l \in [w-1] \\ 0, & \text{otherwise} \end{cases} \quad (6)$$

The output $\mathbf{Y} \in \mathbb{R}^{c_{out} \times n \times n}$ of the convolution operation is given by:

$$\mathbf{Y}_{c,r,s} = \sum_{d=0}^{c_{in}-1} \sum_{k=0}^{n-1} \sum_{l=0}^{n-1} \mathbf{X}_{d,r+k,s+l} \mathbf{K}_{c,d,k,l}$$

We construct a matrix \mathbf{J} of dimensions $c_{out}n^2 \times c_{in}n^2$ as follows:

$$\mathbf{J} = \begin{bmatrix} \mathbf{B}^{(0,0)} & \mathbf{B}^{(0,1)} & \dots & \mathbf{B}^{(0,c_{in}-1)} \\ \mathbf{B}^{(1,0)} & \mathbf{B}^{(1,1)} & \dots & \mathbf{B}^{(1,c_{in}-1)} \\ \vdots & \vdots & \ddots & \vdots \\ \mathbf{B}^{(c_{out}-1,0)} & \mathbf{B}^{(c_{out}-1,1)} & \dots & \mathbf{B}^{(c_{out}-1,c_{in}-1)} \end{bmatrix}, \quad \mathbf{B}^{(c,d)} = \text{circ}(\mathbf{K}_{c,d,;,:})$$

By inspection we can see that:

$$\text{vec}(\mathbf{Y}) = \mathbf{J} \text{vec}(\mathbf{X})$$

This directly implies that \mathbf{J} is the jacobian of $\text{vec}(\mathbf{Y})$ with respect to $\text{vec}(\mathbf{X})$ and our goal is to find a differentiable upper bound on the largest singular value of \mathbf{J} .

From Sedghi et al.[21], we know that singular values of \mathbf{J} are given by:

$$\sigma(\mathbf{J}) = \bigcup_{j \in [n-1], k \in [n-1]} \sigma(\mathbf{G}^{(j,k)}) \quad (7)$$

where each $\mathbf{G}^{(j,k)}$ is a matrix of dimensions $c_{out} \times c_{in}$ and each element of $\mathbf{G}^{(j,k)}$ is given by:

$$\mathbf{G}_{c,d}^{(j,k)} = (\mathbf{F}^T \mathbf{K}_{c,d,:} \mathbf{F})_{j,k}, \quad c \in [c_{out} - 1], d \in [c_{in} - 1] \quad (8)$$

Using equation (7), we can directly observe that a differentiable upper bound over the largest singular value of $\mathbf{G}^{(j,k)}$ that is independent of j and k will give an desired upper bound. We will next derive the same.

Using equation (8), we can rewrite $\mathbf{G}_{c,d}^{(j,k)}$ as:

$$\mathbf{G}_{c,d}^{(j,k)} = (\mathbf{F}^T \mathbf{K}_{c,d,:} \mathbf{F})_{j,k} = (\mathbf{F}_{:,j})^T \mathbf{K}_{c,d,:} \mathbf{F}_{:,k} \quad (9)$$

Using equation (6), we know that $\mathbf{K}_{c,d,:}$ is a sparse matrix of size $n \times n$ with only the top-left block of size $h \times w$ that is non-zero. We take the first h rows and w columns of $\mathbf{K}_{c,d,:}$ i.e $\mathbf{K}_{c,d;h,w}$, first h elements of $\mathbf{F}_{:,j}$ i.e $\mathbf{F}_{:h,j}$ and first w elements of $\mathbf{F}_{:,k}$ i.e $\mathbf{F}_{:w,k}$. We have the following equality:

$$\mathbf{G}_{c,d}^{(j,k)} = (\mathbf{F}_{:,j})^T \mathbf{K}_{c,d,:} \mathbf{F}_{:,k} = (\mathbf{F}_{:h,j})^T \mathbf{K}_{c,d;h,w} \mathbf{F}_{:w,k} = (\mathbf{F}_{:h,j})^T \mathbf{L}_{c,d,:} \mathbf{F}_{:w,k} \quad (10)$$

Now consider a block matrix \mathbf{R} of dimensions $c_{out}h \times c_{in}w$ given by:

$$\mathbf{R} = \begin{bmatrix} \mathbf{K}_{0,0;h,w} & \mathbf{K}_{0,1;h,w} & \cdots & \mathbf{K}_{0,c_{in}-1;h,w} \\ \mathbf{K}_{1,0;h,w} & \mathbf{K}_{1,1;h,w} & \cdots & \mathbf{K}_{1,c_{in}-1;h,w} \\ \vdots & \vdots & \ddots & \vdots \\ \mathbf{K}_{c_{out}-1,0;h,w} & \mathbf{K}_{c_{out}-1,1;h,w} & \cdots & \mathbf{K}_{c_{out}-1,c_{in}-1;h,w} \end{bmatrix}$$

Using equation (6), we can write \mathbf{R} as follows:

$$\mathbf{R} = \begin{bmatrix} \mathbf{L}_{0,0,:} & \mathbf{L}_{0,1,:} & \cdots & \mathbf{L}_{0,c_{in}-1,:} \\ \mathbf{L}_{1,0,:} & \mathbf{L}_{1,1,:} & \cdots & \mathbf{L}_{1,c_{in}-1,:} \\ \vdots & \vdots & \ddots & \vdots \\ \mathbf{L}_{c_{out}-1,0,:} & \mathbf{L}_{c_{out}-1,1,:} & \cdots & \mathbf{L}_{c_{out}-1,c_{in}-1,:} \end{bmatrix} \quad (11)$$

Thus the block in c^{th} row and d^{th} column of \mathbf{R} is the $h \times w$ matrix $\mathbf{L}_{c,d,:}$.

Consider two matrices: $\mathbf{I}_{c_{out}} \otimes (\mathbf{F}_{:h,j})^T$ of dimensions $c_{out} \times c_{out}h$, $\mathbf{I}_{c_{in}} \otimes \mathbf{F}_{:w,k}$ of dimensions $c_{in}w \times c_{in}$.

Using equations (9) and (11), we can see that:

$$\mathbf{G}^{(j,k)} = (\mathbf{I}_{c_{out}} \otimes (\mathbf{F}_{:h,j})^T) \mathbf{R} (\mathbf{I}_{c_{in}} \otimes \mathbf{F}_{:w,k})$$

Taking the spectral norm of both sides:

$$\begin{aligned} \|\mathbf{G}^{(j,k)}\|_2 &= \|(\mathbf{I}_{c_{out}} \otimes (\mathbf{F}_{:h,j})^T) \mathbf{R} (\mathbf{I}_{c_{in}} \otimes \mathbf{F}_{:w,k})\|_2 \\ \|\mathbf{G}^{(j,k)}\|_2 &\leq \|(\mathbf{I}_{c_{out}} \otimes (\mathbf{F}_{:h,j})^T)\|_2 \|\mathbf{R}\|_2 \|(\mathbf{I}_{c_{in}} \otimes \mathbf{F}_{:w,k})\|_2 \end{aligned}$$

Using $\|\mathbf{A} \otimes \mathbf{B}\|_2 = \|\mathbf{A}\|_2 \|\mathbf{B}\|_2$ and since both $\|\mathbf{I}_{c_{out}}\|_2$ and $\|\mathbf{I}_{c_{in}}\|_2$ are 1:

$$\|\mathbf{G}^{(j,k)}\|_2 \leq \|\mathbf{F}_{:h,j}\|_2 \|\mathbf{R}\|_2 \|\mathbf{F}_{:w,k}\|_2$$

Further note that since $\mathbf{F}_{j,k} = \omega^{jk}$, we have $\|\mathbf{F}_{:h,j}\|_2 = \sqrt{h}$ and $\|\mathbf{F}_{:w,k}\|_2 = \sqrt{w}$.

$$\|\mathbf{G}^{(j,k)}\|_2 \leq \sqrt{hw} \|\mathbf{R}\|_2$$

Alternative inequality: Note that equation (10) can also be written by taking the transpose of the scalar $(\mathbf{F}_{:h,j})^T \mathbf{L}_{:,c,d} \mathbf{F}_{:w,k}$:

$$\mathbf{G}_{c,d}^{(j,k)} = (\mathbf{F}_{:h,j})^T \mathbf{L}_{c,d,:} \mathbf{F}_{:w,k} = (\mathbf{F}_{:w,k})^T (\mathbf{L}_{c,d,:})^T \mathbf{F}_{:h,j} \quad (12)$$

Now consider a block matrix \mathbf{S} of dimensions $c_{out}w \times c_{in}h$ given by:

$$\mathbf{S} = \begin{bmatrix} (\mathbf{L}_{0,0,:})^T & (\mathbf{L}_{0,1,:})^T & \cdots & (\mathbf{L}_{0,c_{in}-1,:})^T \\ (\mathbf{L}_{1,0,:})^T & (\mathbf{L}_{1,1,:})^T & \cdots & (\mathbf{L}_{1,c_{in}-1,:})^T \\ \vdots & \vdots & \ddots & \vdots \\ (\mathbf{L}_{c_{out}-1,0,:})^T & (\mathbf{L}_{c_{out}-1,1,:})^T & \cdots & (\mathbf{L}_{c_{out}-1,c_{in}-1,:})^T \end{bmatrix} \quad (13)$$

For \mathbf{S} the block in c^{th} row and d^{th} column of \mathbf{R} is the $w \times h$ matrix $(\mathbf{I}_{c,d,:})^T$. Consider two matrices: $\mathbf{I}_{c_{out}} \otimes (\mathbf{F}_{:w,k})^T$ of dimensions $c_{out} \times c_{out}w$, $\mathbf{I}_{c_{in}} \otimes \mathbf{F}_{:h,j}$ of dimensions $c_{in}h \times c_{in}$. Using equations (9) and (11), we again have:

$$\mathbf{G}^{(j,k)} = (\mathbf{I}_{c_{out}} \otimes (\mathbf{F}_{:w,k})^T) \mathbf{S} (\mathbf{I}_{c_{in}} \otimes \mathbf{F}_{:h,j})$$

Taking the spectral norm of both sides and using the same procedure that we used for \mathbf{R} , we get the following inequality:

$$\|\mathbf{G}^{(j,k)}\|_2 \leq \sqrt{hw} \|\mathbf{S}\|_2$$

Using equations (11) and (13), we can see that both \mathbf{R} and \mathbf{S} are independent of j,k and input size n . Furthermore, we can differentiate $\|\mathbf{R}\|_2$ by computing the singular vectors \mathbf{u} and \mathbf{v} that satisfy:

$$\mathbf{R}\mathbf{v} = \|\mathbf{R}\|_2 \mathbf{u}$$

The derivative of $\|\mathbf{R}\|_2$ with respect to \mathbf{R} is then given by:

$$\nabla_{\mathbf{R}} \|\mathbf{R}\|_2 = \mathbf{u}\mathbf{v}^T$$

$\|\mathbf{R}\|_2$, \mathbf{u} and \mathbf{v} can be computed using power iteration. Derivative of $\|\mathbf{S}\|_2$ with respect to \mathbf{S} can be computed similarly. ■

B Effect of increasing β on singular values

Filter shape	β values							
	0	0.0006	0.0008	0.001	0.0012	0.0014	0.0016	0.0018
$16 \times 3 \times 3 \times 3$	37.96	11.05	9.13	8.2	7.28	8.66	7.06	5.57
$16 \times 16 \times 3 \times 3$	22.23	5.89	5.08	5.26	5.19	6.17	3.41	3.27
$16 \times 16 \times 3 \times 3$	25.33	5.69	4.87	4.9	4.75	5.80	3.26	3.27
$16 \times 16 \times 3 \times 3$	25.29	5.28	4.74	4.08	2.89	6.60	3.72	2.32
$16 \times 16 \times 3 \times 3$	21.66	4.99	4.36	3.64	2.64	5.81	3.61	2.25
$16 \times 16 \times 3 \times 3$	20.15	4.92	3.89	4.61	2.53	3.13	0.07	2.4
$16 \times 16 \times 3 \times 3$	16.36	4.37	3.52	4.08	2.34	2.60	0.07	2.14
$16 \times 16 \times 3 \times 3$	15.39	5.39	5.65	3.15	4.1	4.72	2.31	1.69
$16 \times 16 \times 3 \times 3$	14.67	4.38	4.61	2.32	3.52	3.66	2.37	1.57
$16 \times 16 \times 3 \times 3$	19.26	7.41	6.28	4.96	3.57	0.13	5.38	3.19
$16 \times 16 \times 3 \times 3$	14.60	5.77	4.84	4.01	2.68	0.09	4.31	2.64
$32 \times 16 \times 3 \times 3$	23.24	8.53	8.09	7.06	6.24	6.30	6.4	6.61
$32 \times 32 \times 3 \times 3$	22.19	9.65	9.57	7.99	7.27	7.12	7.72	7.82
$32 \times 32 \times 3 \times 3$	17.97	7.61	7.52	6.32	4.72	5.25	5.06	2.57
$32 \times 32 \times 3 \times 3$	16.76	6.83	6.29	5.38	4.12	4.48	4.48	2.22
$32 \times 32 \times 3 \times 3$	17.62	8.31	6.2	6.73	4.06	5.23	5.65	3.21
$32 \times 32 \times 3 \times 3$	15.7	7.24	5.23	5.5	3.42	4.45	4.73	2.8
$32 \times 32 \times 3 \times 3$	15.82	8.34	5.42	5.29	4.86	5.41	5.03	4.11
$32 \times 32 \times 3 \times 3$	15.83	6.99	4.48	4.47	4.02	4.62	4.24	3.56
$32 \times 32 \times 3 \times 3$	18.46	8.1	6.03	5.31	5.91	5.64	4.83	6.24
$32 \times 32 \times 3 \times 3$	17.75	7.08	5.17	4.53	4.98	4.61	4.15	5.31
$64 \times 32 \times 3 \times 3$	23.57	12.21	10.97	10.41	10.84	10.15	9.7	10.31
$64 \times 64 \times 3 \times 3$	22.97	13.2	12.23	11.72	12.55	11.36	11.14	12.39
$64 \times 64 \times 3 \times 3$	22.35	12.18	11.71	11.13	10.53	10.57	10.2	10.43
$64 \times 64 \times 3 \times 3$	22.02	11.28	10.95	10.43	9.94	9.94	9.52	9.55
$64 \times 64 \times 3 \times 3$	20.91	12.09	11.7	11.07	10.47	10.85	9.87	9.81
$64 \times 64 \times 3 \times 3$	21.77	10.85	10.51	9.81	9.6	9.62	8.56	8.43
$64 \times 64 \times 3 \times 3$	19.63	11.97	11.56	10.28	10.98	10.02	9.32	8.69
$64 \times 64 \times 3 \times 3$	17.61	10	10.03	8.81	9.63	8.26	7.57	7.35
$64 \times 64 \times 3 \times 3$	16.67	10.34	11.61	10.26	10.93	8.64	8.05	8.56
$64 \times 64 \times 3 \times 3$	17.81	8.16	8.73	7.68	8.18	6.61	6.07	6.49
10×64	12.43	10.79	10.55	10.53	10.11	10.14	9.64	9.39

Table 5: Effect of increasing β on the bounds ($\sqrt{hw}\|\mathbf{R}\|_2$) of each layer

C Comparison between $\sqrt{hw}\|\mathbf{R}\|_2$ and $\sqrt{hw}\|\mathbf{S}\|_2$

Filter shape	$\sqrt{hw}\ \mathbf{R}\ _2$	$\sqrt{hw}\ \mathbf{S}\ _2$
$64 \times 3 \times 7 \times 7$	47.292	46.373
$64 \times 64 \times 3 \times 3$	9.545	9.612
$64 \times 64 \times 3 \times 3$	6.571	6.296
$64 \times 64 \times 3 \times 3$	8.921	8.712
$64 \times 64 \times 3 \times 3$	5.402	5.520
$128 \times 64 \times 3 \times 3$	6.994	6.923
$128 \times 128 \times 3 \times 3$	7.447	7.384
$128 \times 128 \times 3 \times 3$	6.779	7.180
$128 \times 128 \times 3 \times 3$	7.571	7.716
$256 \times 128 \times 3 \times 3$	8.580	8.454
$256 \times 256 \times 3 \times 3$	8.195	8.067
$256 \times 256 \times 3 \times 3$	8.062	8.127
$256 \times 256 \times 3 \times 3$	9.910	9.757
$512 \times 256 \times 3 \times 3$	11.238	11.003
$512 \times 512 \times 3 \times 3$	10.979	10.653
$512 \times 512 \times 3 \times 3$	20.218	19.903
$512 \times 512 \times 3 \times 3$	7.834	7.990

Table 6: Comparison between our proposed bounds ($\sqrt{hw}\|\mathbf{R}\|_2$, $\sqrt{hw}\|\mathbf{S}\|_2$)

Using Theorem 1, we know that both $\sqrt{hw}\|\mathbf{R}\|_2$ and $\sqrt{hw}\|\mathbf{S}\|_2$ are upper bounds on the largest singular values of the convolution layer. In Table 6, we compare the difference between the two bounds on a Resnet-18 convolutional neural network pretrained on Imagenet and observe small difference.

D Comparison between our upper bound, exact spectral norm and heuristic

Filter shape	Spectral norm estimates			Running time (in seconds)		
	Exact method [21]	Heuristic [19, 20]	Upper bound (Ours)	Exact	Heuristic	Ours
$64 \times 3 \times 7 \times 7$	15.917	4.128	46.373	3.166	0.003	0.280
$64 \times 64 \times 3 \times 3$	6.006	3.109	9.545	75.481	0.004	0.007
$64 \times 64 \times 3 \times 3$	5.341	2.163	6.296	80.777	0.003	0.008
$64 \times 64 \times 3 \times 3$	6.999	2.934	8.712	80.213	0.004	0.008
$64 \times 64 \times 3 \times 3$	3.816	1.937	5.402	81.744	0.004	0.008
$128 \times 64 \times 3 \times 3$	4.706	1.978	6.923	30.634	0.007	0.010
$128 \times 128 \times 3 \times 3$	5.722	2.405	7.284	71.551	0.010	0.027
$128 \times 128 \times 3 \times 3$	4.410	2.282	6.779	72.608	0.010	0.026
$128 \times 128 \times 3 \times 3$	4.885	2.965	7.571	72.885	0.010	0.026
$256 \times 128 \times 3 \times 3$	7.395	2.890	8.454	28.750	0.029	0.043
$256 \times 256 \times 3 \times 3$	6.583	2.679	8.067	68.778	0.056	0.154
$256 \times 256 \times 3 \times 3$	6.361	2.524	8.062	69.220	0.055	0.151
$256 \times 256 \times 3 \times 3$	7.677	3.658	9.757	68.673	0.055	0.151
$512 \times 256 \times 3 \times 3$	9.991	3.834	11.003	32.103	0.192	0.287
$512 \times 512 \times 3 \times 3$	9.094	3.970	10.653	89.484	0.355	0.988
$512 \times 512 \times 3 \times 3$	17.600	7.304	19.903	89.129	0.345	0.938
$512 \times 512 \times 3 \times 3$	7.479	2.752	7.834	90.017	0.352	0.972

Table 7: Comparison between the exact spectral norm of the jacobian $\|\mathbf{J}\|_2$ (computed using Sedghi et al. [21]), the heuristic method [19, 20] and our proposed bound $\min(\sqrt{hw}\|\mathbf{R}\|_2, \sqrt{hw}\|\mathbf{S}\|_2)$ for a Resnet-18 network pretrained on Imagenet[25]. The heuristic is always significantly smaller than the exact spectral norm. However, $\min(\sqrt{hw}\|\mathbf{R}\|_2, \sqrt{hw}\|\mathbf{S}\|_2)$ is within 1.5 times the exact spectral norm $\|\mathbf{J}\|_2$ (except the first layer). All running times were computed on the CPU using tensorflow.